Insights from long term follow-up of a girl with adrenal insufficiency and sphingosine-1-phosphate lyase deficiency

Avinaash Maharaj[a], Tülay Güran[b], Federica Buonocore[c], John C. Achermann[c], Louise Metherell[a], Rathi Prasad*[a], Semra Çetinkaya*[d]

[a] Centre for Endocrinology, William Harvey Research Institute, John Vane Science Centre, Queen Mary, University of London, Charterhouse Square, London, United Kingdom

[b] Marmara University, School of Medicine, Department of Paediatric Endocrinology and Diabetes, Istanbul, Turkey

[c] Genetics and Genomic Medicine Research and Teaching Department, UCL Great Ormond Street Institute of Child Health, University College London, London, UK

[d] Health Sciences University, Dr. Sami Ulus Obstetrics and Gynecology, Children's Health and Disease Education and Research Hospital, Ankara, Turkey.

*Denotes equal contribution

Disclosure statement: The authors have nothing to disclose.

Corresponding Author:

Dr Rathi Prasad

Centre for Endocrinology,

William Harvey Research Institute, Queen Mary University of London

Charterhouse Square, London, EC1M 6BQ

Email: r.prasad@qmul.ac.uk

ORCID: 0000-0001-6360-7246

Abstract

Introduction: Sphingosine-1-phosphate lyase (SGPL1) insufficiency syndrome (SPLIS) is a multi-systemic disorder which, in the main, incorporates steroid resistant nephrotic syndrome and primary adrenal insufficiency (PAI).

Case Presentation: We present a young girl with a novel homozygous variant in *SGPL1*; p.D350G, with PAI in the absence of nephrotic syndrome. In the course of 15 years of follow up she has further developed primary hypothyroidism and whilst she has progressed through puberty appropriately, ovarian calcifications were noted on imaging. The p.D350G variant results in reduced protein expression of SGPL1. We demonstrate that CRISPR engineered knockout of *SGPL1* in human adrenocortical (H295R) cells abrogates cortisol production. Furthermore, whilst wild-type SGPL1 is able to rescue cortisol production in this *in vitro* model of adrenal disease, this is not observed with the p.D350G mutant.

Conclusion: SGPL1 deficiency should be considered in the differential diagnosis of PAI with close attention paid to evolving disease on follow up.

3

1   Introduction

2   Sphingosine-1-phosphate lyase (SGPL1) insufficiency syndrome (SPLIS, Nephrotic Syndrome, type 14;

3   NPHS14; MIM 617575) is unique amongst disorders of sphingolipid metabolism due to its multi-

4   endocrine pathology. In addition to steroid resistant nephrotic syndrome, ichthyosis and neurological

5   disease, which are seen in some of the other sphingolipidoses, SPLIS also incorporates primary

6   adrenal insufficiency (PAI) and primary hypothyroidism(1).Furthermore, primary hypogonadism has

7   been reported in affected boys(2–4). Delineating a clear genotype-phenotype correlation in this

8   disorder is complicated by marked phenotypic heterogeneity since mutation type, domain topology

9   and perceived enzyme activity do not always predict disease severity.

10   We report a novel variant in *SGPL1* in a patient presenting with early-onset primary adrenal failure

11   and subsequent hypothyroidism, in the absence of renal pathology. Early identification of this

12   syndrome enables ongoing surveillance for the emergence of other disease features allowing timely

13   and appropriate interventions.

14   Case Presentation

15   A Turkish female infant from a consanguineous kindred initially presented at the age of 9 months

16   with fever, seizures, generalised hyperpigmentation and ichthyosis. Biochemical investigations

17   revealed marked hypocortisolaemia (20.9nmol/L) associated with high plasma ACTH (4500pmol/L)

18   levels. MR imaging revealed increased bilateral parieto-occipital uptake suggestive of

19   meningoencephalitis. Mineralocorticoid deficiency as evidenced by raised plasma renin

20   concentration (55pg/ml) was also identified and hydrocortisone and fludrocortisone replacement

21   were started. The patient's recovery was complicated by the development of cortical visual

22   impairment. Since diagnosis, the patient was noted to have steadily increasing TSH levels warranting

23   a diagnosis of primary hypothyroidism treated with L-thyroxine (shown in Table 1). At the age of 10

4

24 years, during routine follow-up, a palpable anterior neck swelling was noted. Ultrasonography

25 revealed a nodular 13x13x5mm infra-hyoid lesion, whilst thyroid lobe architecture was

26 homogeneous and otherwise unremarkable. Post-operative pathological evaluation was suggestive

27 of a benign thyroglossal cyst with psammomatous calcification.   The patient has since entered

28 puberty with normal ovarian reserve (anti-müllerian hormone concentration of 4.93ng/mL, Normal

29 range: 0.86-10.45) despite detection of ovarian calcifications on imaging conducted for irregular

30 periods(shown in Fig. 1). Renal function, including assessment of urine protein creatinine ratio,

31 during surveillance following diagnosis has been normal (shown in Table 1). Whilst she was born

32 small for gestational age (SGA) at term (birthweight -2.35 SDS), she had further evidence of growth

33 failure with a final height at -3.67 SDS and parent adjusted height of -2.40 SDS, despite IGF-1 levels

34 within normal range.

35 **Materials and Methods**

36 **Variant detection and confirmation**

37 A homozygous *SGPL1* variant c.1049A>G;p.D350G was found on whole exome sequencing (WES) and

38 confirmed by Sanger sequencing using primers amplifying exon 11 of *SGPL1* (Forward – 5'-

39 CATCTTTCCACCCATGTCT-3' and Reverse – 5'- GTGACGGCAAAGAGAGAGT-3'). Pathogenicity of the

40 missense variant was evaluated using a combination of predictive tools: Sorting Intolerant from

41 Tolerant (SIFT)(5), Polymorphism Phenotyping v2 (PolyPhen2)(6), Combined Annotation Dependent

42 Depletion (CADD)(7), Mutation taster(8) and Protein Variation Effect Analyser (PROVEAN)(9).

43 **Protein structure modelling and thermo-stability analysis**

44 Protein 3D modelling of PDB (Protein Data Bank) SGPL1 crystal structure (4Q6R)(10) was performed

45 using the tool PyMOL (Schrodinger, LLC. 2010. The PyMOL Molecular Graphics System, Version X.X.)

46 with thermo-stability of mutant protein assessed using computational platforms: DynaMut(11), I-

47 Mutant2.0-SEQ(12), iSTABLE2.0 (MUpro_SVM, MUpro_NN)(13), iPTREE-STAB(14), and SDM(15).

48 **Site directed mutagenesis**

49 Site-directed mutagenesis of an *SGPL1* (NM_003901) Human Tagged ORF Clone (ORIGENE,

50 RC208705) was performed using the QuikChange II XL Site-Directed Mutagenesis Kit (Agilent,

51 200521) according to the manufacturer's instructions. Primers for generation of four specific mutants

52 in SGPL1 (p.D350G, p.N171D, p.Y15C, and p.F545del) were designed using the online tool

53 https://www.agilent.com/store/primerDesignProgram.jsp.

54 **CRISPR-Cas9 engineered knockout of *SGPL1* in an adrenocortical cell line**

55 CRISPR gene editing was achieved utilising the protocol outlined by Ran *et. al*(16) and previously

56 published single guide RNA (sgRNA) sequences(17). The sgRNA oligos were then cloned into

57 pSpCas9(BB)-2A-GFP (PX458), a gift from Feng Zhang (Addgene plasmid # 48138;

58 http://n2t.net/addgene:48138; RRID:Addgene_48138)(16) and introduced into NCI-H295R [H295R]

59 (ATCC® CRL-2128™) adrenocortical cells via transfection using Lipofectamine™ 3000 according to

60 manufacturer's instructions. After 72 hours, GFP-positive cells were cell sorted by FACS

61 (fluorescence-activated cell sorting) into prepared 96-well plates, to ensure single cell clonal

62 expansion. Colonies were expanded and genotyped after 4-6 weeks.

63 **Western blotting**

64 *SGPL1* knockout H295R cells were seeded into 6 well culture plates and transfected with either wild

65 type SGPL1 or mutant construct using Lipofectamine 3000® reagent (Thermo Fisher Scientific). After

66 48h, whole cell lysates were prepared by addition of RIPA buffer (Sigma Aldrich) supplemented with

67 protease and phosphatase inhibitor tablets (Roche). Protein concentrations were quantified using a

68 Bradford protein assay (Bio-Rad) and lysates denatured by addition of Laemmli sample buffer 2X

6

69　(Sigma Aldrich) and boiled for 5 minutes at 98°C. 20µg of protein was loaded into the wells of a 4-

70　20% SDS-PAGE gel (Novex) prior to electrophoretic separation using MOPS buffer. Protein transfer to

71　nitrocellulose membrane was achieved by electro-blotting at 15V for 45 minutes. The membrane was

72　blocked with 5% fat free milk in TBS/0.1% Tween-20 and left to gently agitate for 1 hour. Primary

73　antibody (Human SGPL1 Antibody; AF5535, R&D Systems; RRID:AB_2188674) was added at a

74　concentration of 1:1000 with mouse anti-Actin beta monoclonal antibody (Abcam, ab6276,

75　RRID:AB_2223210) at a concentration of 1:10,000 used as a housekeeping control. Primary antibody

76　incubation was left overnight at 4°C with gentle agitation. The membrane was then washed for 5

77　minutes (three times) with Tris Buffered saline-Tween20 (TBST). Secondary anti-mouse (IRDye®

78　800CW Goat anti-Mouse IgG; RRID:AB_10793856) and anti-goat (IRDye® 680RD Donkey anti-Goat

79　IgG; RRID:AB_10956736) antibodies were added at a concentration of 1:5000 to blocking buffer and

80　the membrane incubated at 37°C for 60 – 90 minutes. The membrane was subsequently washed

81　three times (5 minutes each) with TBST and visualized with the LI-COR Image Studio software for

82　immune-fluorescent detection.

83　**Forskolin stimulation of adrenocortical cells**

84　*SGPL1* WT and knockout H295R cells were seeded into 6 well plates at a density of 2.5×10^6 cells per

85　well and cultured in serum-free media. Additionally, discrete wells were transfected (using

86　Lipofectamine™ 3000 according to manufacturer's instructions) with *SGPL1* ORF clone (WT) and

87　p.D350G mutant constructs. Cells were then stimulated with 10 µM forskolin for 24 hours followed

88　by harvesting of media and protein extraction from cells. Forskolin treatment, as a surrogate to ACTH

89　stimulation, has been shown to alter expression of steroidogenic enzymes in NCI-H295R cells leading

90　to an almost 25-fold increase in cortisol production[18]. Cortisol levels in supernatants were analysed

91　on a Roche Modular E170 automated immunoassay analyser using electrochemiluminescent

92　detection as per previous publication[19]. Cortisol measurements were normalised to protein levels

7

93   following protein quantification by Bradford assay. Data are presented as the mean ± SD of three

94   experiments.

95   **Statistics**

96   Statistical analysis was performed using a 2-tailed Student's t test to generate P values. P values less

97   than or equal to 0.05 were considered significant. Data are presented as mean ± SD where error bars

98   are shown.

99   **Results**

100   Whole exome sequencing of patient DNA revealed a novel homozygous variant in *SGPL1*

101   (chr10:72631733A>G, c.1049A>G), which was confirmed by Sanger sequencing. Multiple protein

102   sequence alignment across several mammalian species showed evolutionary conservation of the

103   aspartic acid at position 350 of SGPL1 (shown in Fig. 2a). Both parents were heterozygous for this

104   variant (shown in Fig. 2b and c). The concordance amongst predictive platforms in assigning

105   pathogenicity of this variant was high, with p.D350G predicted deleterious across the five

106   computational platforms utilised. Protein modelling using PyMOL (shown in Fig. 3a and b) and

107   DynaMut (shown in Fig. 3c) demonstrated significant alterations to protein conformation, with

108   substitution of glycine for aspartic acid at position 350 predicted to lead to thermal instability (ΔΔG <

109   0) and increased molecule flexibility (shown in Fig. 4a and b). The effect of this variant was evaluated

110   alongside other known published mutations (p.N171D, p.Y15C, and p.F545del)[2,20,21]. Patients

111   with *SGPL1* mutations p.N171D and p.F545del presented with both PAI and nephrotic syndrome,

112   whilst the patient with p.Y15C variant was atypical, presenting with neurological disease alone.

113   SGPL1 protein levels probed by immunoblotting revealed decreased expression of p.D350G and the

114   other mutants when compared to wild type; with the highest expression in p.Y15C correlating with

115   the milder/atypical phenotype of this patient (shown in Fig. 5a). To further test the function of the

116   p.D350G variant, CRISPR engineered *SGPL1*-knockout (KO) human adrenocortial (H295R) cells were

8

117 utilised as a vehicle for corticosteroid measurement following forskolin stimulation. Basally, both WT

118 and KO cells showed minimal cortisol output but following forskolin treatment, *SGPL1*-KO cells

119 showed no response compared to a brisk response in WT cells (shown in Fig. 5b). Cortisol

120 measurement of cell sera following transfection with *SGPL1*-WT or the p.D350G variant construct

121 revealed an inability of the mutant to rescue cortisol output in contrast to the *SGPL1*-WT construct

122 (shown in Fig. 5b).

123 **Discussion:**

124 Mutations in *SGPL1* often produce highly variable clinical phenotypes, ranging from severe multi-

125 systemic disease, associated with fetal hydrops and early mortality, to isolated single organ

126 disease(2–4,22). This further complicates establishing a strong genotype-phenotype correlation for

127 SPLIS. Patients with this disorder of sphingolipid metabolism almost invariably present with

128 congenital or steroid resistant nephrotic syndrome often progressing to end-stage renal disease(23).

129 Our patient, with the p.D350G mutation in a highly conserved domain of the lyase, is one of the

130 exceptions, presenting primarily with adrenal failure. She had ichthyosis and thyroid disease, also

131 described in this rare syndrome. Four other individuals with SPLIS in the literature have presented

132 with adrenal insufficiency without concomittant nephrotic disease, all with the p.R222Q *SGPL1*

133 mutation(2,24). Whilst two of these individuals had other clinical features associated with the

134 syndrome including lymphopenia and seizures(2,24), two presented with adrenal disease alone(2),

135 highlighting the importance of considering SGPL1 in the differential diagnosis of isolated primary

136 adrenal insufficiency.

137 Impaired steroid production in SPLIS is also evident in the gonad, with approximately a third of

138 affected males presenting with primary gonadal insufficiency(2–4,20,25,26). Ovarian pathology has

139 not been previously reported. An impact on puberty has not been widely studied in this condition,

140 particularly in girls, often precluded by the high early-childhood mortality associated with SPLIS.

9

141 Certainly both sexes of *Sgpl1*^{-/-} mouse models are sterile indicating an effect of SGPL1 deficiency on

142 both ovarian and testicular function(27), likely due to an accumulation of sphingosine-1-

143 phosphate(27,28). In *Sgpl1*^{-/-} mice, postnatal reduction in testis size, loss of spermatocytes in the

144 testis cords and loss of spermatogenesis are observed together with reduced expression of

145 steroidogenic enzymes. Similarly *Sgpl1*^{-/-} postnatal ovaries have reduced steroidogenic enzyme

146 expression and are noted to be smaller with fewer antral follicles and corpora lutea(27). Our patient

147 demonstrated normal pubertal development; this has also been described in one other female

148 patient in the literature with typical SPLIS features(2). However, our patient has developed non-

149 neoplastic ovarian calcifications of unknown significance, which do not at this stage appear to be

150 impeding gonadal function. There is clearly a need for surveillance of patients of both sexes

151 throughout puberty and beyond, given the potential risk of evolving gonadal insufficiency.

152 Interestingly, adrenal calcifications have been reported in several SPLIS patients(3,4,20,22,25). Whilst

153 the exact mechanism for this is unknown, adrenal calcifications seen with lysosomal acid lipase

154 deficiency or Wolman disease are due to cholesterol and fatty acid deposition within the adrenal

155 cortex(29), suggesting that calcification in this sphingolipidosis may be due to lipid dyshomeostasis.

156 There are no other reports in the SPLIS literature of calcified thyroglossal cysts, as is reported with

157 our patient and this may be an incidental finding unrelated to the syndrome. Our patient was born

158 SGA with further poor growth on follow-up despite normal IGF-1 levels. SGPL1 deficiency in murine

159 models is associated with significant post-natal growth restriction(27), however there is limited data

160 on growth within the SPLIS patient cohort, impeded by high early mortality and lack of follow-up

161 data.

162 Given the high burden of disease and implications of a positive SPLIS diagnosis, *in silico* predictive

163 tools may be useful as an initial step to delineate which variants may be disease-causing although

164 functional testing remains the gold standard in evaluating pathogenicity. Thermodynamic profiling

165 designated p.D350G as a destabilising variant (ΔΔG < 0, shown in Fig. 4a) suggesting that this point

166   mutation renders the protein unstable due in part to loss of hydrogen bonding (Fig. 4b). The

167   mutagenized p.D350G construct exhibited reduced SGPL1 protein expression when compared to wild

168   type SGPL1. Other published variants (p.N171D, p.F545del and p.Y15C)(2,20,21) demonstrated

169   similarly reduced expression, with the exception of p.Y15C. The subtle reduction in protein, mirrored

170   the mild phenotype of isolated neurological disease seen with the p.Y15C variant and increased

171   protein stability on thermodynamic profiling prediction; indeed the absence of typical features of

172   SPLIS in this patient were interpreted with the caveat that they may be attributable to another

173   genetic defect(21).

174   The degree of residual enzymatic activity should theoretically predict phenotypic severity. Prasad *et*

175   *al.* expressed mutagenized constructs for missense variant p.R222Q and in-frame deletion, p.F545del

176   in *Sgpl1*$^{-/-}$ mouse embryonic fibroblasts and measured hexadecanal production as a surrogate marker

177   of lyase activity(2). Despite significantly abrogated enzyme activity for both pathogenic variants, the

178   phenotype of each patient was different. p.F545del rendered a more striking phenotype with rapid

179   disease progression while p.R222Q demonstrated marked variability amongst affected family

180   members harbouring the same mutation(2).

181   Reduced steroidogenic output associated with mitochondrial dysfunction is observed in SPLIS

182   patient-derived dermal fibroblasts with disordered sphingolipid metabolism(30). We have

183   established *SGPL1*-KO H295R cells as an *in vitro* adrenal model of the disease. Despite forskolin

184   stimulation for 24 hours, *SGPL1* KO H295R cells demonstrated an impaired cortisol response when

185   compared to control. Forskolin stimulation of the KO cells transfected with the mutagenized *SGPL1*

186   D350G construct, similarly demonstrated diminished cortisol responsiveness when compared to a

187   wild type rescue. Interrogation of this *in vitro* model disease is currently underway to explore the

188   precise impact that SGPL1 deficiency has on steroidogenesis.

11

189   In conclusion, our patient presented atypically with adrenal disease in the absence of nephrotic

190   syndrome, despite the p.D350G variant resulting in markedly reduced SGPL1 expression. A clear

191   functional effect was demonstrated in an *in vitro* adrenal model of disease. Genetic modifiers and

192   other tissue-specific pathogenic mechanisms including secondary effects of sphingolipid

193   accumulation and dysregulated signalling pathways may account for the lack of phenotypic

194   uniformity seen with ablation of SGPL1 activity. The published literature suggests that the prognosis

195   for these patients is poor with just under 50% mortality in childhood, the majority of those deaths

196   occurring in the first year of life[20]. Future research will potentially lead to targeted genetic

197   therapies but, for now, a heightened awareness of the syndrome will allow earlier recognition,

198   enabling appropriate and timely intervention targeted towards limiting morbidity and improving

199   quality of life outcomes.

200

201

12

Statement of Ethics

Conflict of Interest Statement

The authors have no conflicts of interest to declare.

Funding Sources

Author Contributions

SC collated patient information. TG, FB and JA carried out initial whole exome sequencing of patient samples. AM carried out all functional studies described. AM, LM and RP designed the studies. All authors were involved in preparing the manuscript.

Data Availability

Some or all datasets generated during and/or analyzed during the current study are not publicly available but are available from the corresponding author on reasonable request.

References

225   1.   Weaver KN, Sullivan B, Hildebrandt F, Strober J, Cooper M, Prasad R, et al. Sphingosine
226   Phosphate Lyase Insufficiency Syndrome. In: Adam MP, Ardinger HH, Pagon RA, Wallace SE, Bean LJ,
227   Mirzaa G, et al., editors. GeneReviews® [Internet]. Seattle (WA): University of Washington, Seattle;
228   1993 [cited 2021 Sep 20]. Available from: http://www.ncbi.nlm.nih.gov/books/NBK562988/

229   2.   Prasad R, Hadjidemetriou I, Maharaj A, Meimaridou E, Buonocore F, Saleem M, et al.
230   Sphingosine-1-phosphate lyase mutations cause primary adrenal insufficiency and steroid-resistant
231   nephrotic syndrome. J Clin Invest. 2017 Mar 1;127(3):942–53.

232   3.   Janecke AR, Xu R, Steichen-Gersdorf E, Waldegger S, Entenmann A, Giner T, et al. Deficiency
233   of the sphingosine-1-phosphate lyase SGPL1 is associated with congenital nephrotic syndrome and
234   congenital adrenal calcifications. Hum Mutat. 2017;38(4):365–72.

235   4.   Bamborschke D, Pergande M, Becker K, Koerber F, Dötsch J, Vierzig A, et al. A novel mutation
236   in sphingosine-1-phosphate lyase causing congenital brain malformation. Brain Dev. 2018 Jun
237   1;40(6):480–3.

238   5.   Ng PC, Henikoff S. SIFT: predicting amino acid changes that affect protein function. Nucleic
239   Acids Res. 2003 Jul 1;31(13):3812–4.

240   6.   Adzhubei IA, Schmidt S, Peshkin L, Ramensky VE, Gerasimova A, Bork P, et al. A method and
241   server for predicting damaging missense mutations. Nat Methods. 2010 Apr;7(4):248–9.

242   7.   Rentzsch P, Witten D, Cooper GM, Shendure J, Kircher M. CADD: predicting the
243   deleteriousness of variants throughout the human genome. Nucleic Acids Res. 2019 Jan
244   8;47(D1):D886–94.

245   8.   Schwarz JM, Rödelsperger C, Schuelke M, Seelow D. MutationTaster evaluates disease-
246   causing potential of sequence alterations. Nat Methods. 2010 Aug;7(8):575–6.

247   9.   Choi Y, Chan AP. PROVEAN web server: a tool to predict the functional effect of amino acid
248   substitutions and indels. Bioinformatics. 2015 Aug 15;31(16):2745–7.

249   10.   Weiler S, Braendlin N, Beerli C, Bergsdorf C, Schubart A, Srinivas H, et al. Orally active 7-
250   substituted (4-benzylphthalazin-1-yl)-2-methylpiperazin-1-yl]nicotinonitriles as active-site inhibitors
251   of sphingosine 1-phosphate lyase for the treatment of multiple sclerosis. J Med Chem. 2014 Jun
252   26;57(12):5074–84.

253   11.   Rodrigues CH, Pires DE, Ascher DB. DynaMut: predicting the impact of mutations on protein
254   conformation, flexibility and stability. Nucleic Acids Res. 2018 Jul 2;46(W1):W350–5.

255   12.   Capriotti E, Fariselli P, Casadio R. I-Mutant2.0: predicting stability changes upon mutation
256   from the protein sequence or structure. Nucleic Acids Res. 2005 Jul 1;33(Web Server issue):W306–
257   10.

14

258 13.   Chen C-W, Lin M-H, Liao C-C, Chang H-P, Chu Y-W. iStable 2.0: Predicting protein thermal
259 stability changes by integrating various characteristic modules. Comput Struct Biotechnol J. 2020 Jan
260 1;18:622–30.

261 14.   Huang L-T, Gromiha MM, Ho S-Y. iPTREE-STAB: interpretable decision tree based method for
262 predicting protein stability changes upon mutations. Bioinformatics. 2007 May 15;23(10):1292–3.

263 15.   Worth CL, Preissner R, Blundell TL. SDM—a server for predicting effects of mutations on
264 protein stability and malfunction. Nucleic Acids Res. 2011 Jul 1;39(Web Server issue):W215–22.

265 16.   Ran FA, Hsu PD, Wright J, Agarwala V, Scott DA, Zhang F. Genome engineering using the
266 CRISPR-Cas9 system. Nat Protoc. 2013 Nov;8(11):2281–308.

267 17.   Gerl MJ, Bittl V, Kirchner S, Sachsenheimer T, Brunner HL, Lüchtenborg C, et al. Sphingosine-
268 1-Phosphate Lyase Deficient Cells as a Tool to Study Protein Lipid Interactions. PLOS ONE. 2016 Apr
269 21;11(4):e0153009.

270 18.   Asif AR, Ljubojevic M, Sabolic I, Shnitsar V, Metten M, Anzai N, et al. Regulation of steroid
271 hormone biosynthesis enzymes and organic anion transporters by forskolin and DHEA-S treatment in
272 adrenocortical cells. Am J Physiol Endocrinol Metab. 2006 Dec;291(6):E1351-1359.

273 19.   Prasad R, Metherell LA, Clark AJ, Storr HL. Deficiency of ALADIN Impairs Redox Homeostasis
274 in Human Adrenal Cells and Inhibits Steroidogenesis. Endocrinology. 2013 Sep;154(9):3209–18.

275 20.   Maharaj A, Theodorou D, Banerjee I (Indi), Metherell LA, Prasad R, Wallace D. A Sphingosine-
276 1-Phosphate Lyase Mutation Associated With Congenital Nephrotic Syndrome and Multiple
277 Endocrinopathy. Front Pediatr [Internet]. 2020 [cited 2020 Apr 14];8. Available from:
278 https://www.frontiersin.org/articles/10.3389/fped.2020.00151/full

279 21.   Martin KW, Weaver N, Alhasan K, Gumus E, Sullivan BR, Zenker M, et al. MRI Spectrum of
280 Brain Involvement in Sphingosine-1-Phosphate Lyase Insufficiency Syndrome. Am J Neuroradiol. 2020
281 Oct 1;41(10):1943–8.

282 22.   Lovric S, Goncalves S, Gee HY, Oskouian B, Srinivas H, Choi W-I, et al. Mutations in
283 sphingosine-1-phosphate lyase cause nephrosis with ichthyosis and adrenal insufficiency. J Clin
284 Invest. 2017 Mar 1;127(3):912–28.

285 23.   Choi Y-J, Saba JD. Sphingosine phosphate lyase insufficiency syndrome (SPLIS):a novel inborn
286 error of sphingolipid metabolism. Adv Biol Regul. 2019 Jan;71:128–40.

287 24.   Settas N, Persky R, Faucz FR, Sheanon N, Voutetakis A, Lodish M, et al. SGPL1 Deficiency: A
288 Rare Cause of Primary Adrenal Insufficiency. J Clin Endocrinol Metab. 2019 May;104(5):1484–90.

289 25.   Taylor VA, Stone HK, Schuh MP, Zhao X, Setchell KD, Erkan E. Disarranged Sphingolipid
290 Metabolism From Sphingosine-1-Phosphate Lyase Deficiency Leads to Congenital Nephrotic
291 Syndrome. Kidney Int Rep [Internet]. 2019 Aug 7 [cited 2019 Sep 15];0(0). Available from:
292 https://www.kireports.org/article/S2468-0249(19)31439-1/

15

293   abstract

294   26.   Zhao P, Liu ID, Hodgin JB, Benke PI, Selva J, Torta F, et al. Responsiveness of sphingosine
295   phosphate lyase insufficiency syndrome to vitamin B6 cofactor supplementation. J Inherit Metab Dis.
296   2020;43(5):1131–42.

297   27.   Schmahl J, Raymond CS, Soriano P. PDGF signaling specificity is mediated through multiple
298   immediate early genes. Nat Genet. 2007 Jan;39(1):52–60.

299   28.   Yuan F, Wang Z, Sun Y, Wei H, Cui Y, Wu Z, et al. Sgpl1 deletion elevates S1P levels,
300   contributing to NPR2 inactivity and p21 expression that block germ cell development. Cell Death Dis.
301   2021 Jun 3;12(6):574.

302   29.   Low G, Irwin GJ, MacPhee GB, Robinson PH. Characteristic imaging findings in Wolman's
303   disease. Clin Radiol Extra. 2004 Oct;59(10):106–8.

304   30.   Maharaj A, Williams J, Bradshaw T, Güran T, Braslavsky D, Casas J, et al. Sphingosine-1-
305   phosphate lyase (SGPL1) deficiency is associated with mitochondrial dysfunction. J Steroid Biochem
306   Mol Biol. 2020 Sep 1;202:105730.

Figure Legends

Table 1. The timeline of pertinent clinical features as they occurred.

Fig. 1. Pelvic ultrasound scan showing areas of calcification (red arrows) in both ovaries.

Fig. 2. a. Partial alignment of SGPL1 protein sequences, showing conservation of aspartic acid (D) at position 350 (green) across several species. Sequence conservation is beneath the alignment, *total conservation, :partial conservation. b. Pedigree of affected patient. Black-filled symbol indicates our patient, homozygous for SGPL1 (c.1049A>G, p.D350G). Grey-filled symbols indicate the parents, heterozygous for the mutation. c. Partial sequence chromatograms of genomic DNA from asymptomatic heterozygote parents and the homozygote patient, showing the base change from A to G in exon 11.

Fig. 3. a. Substitution of the charged aspartic acid for the smaller glycine at codon 350 is demonstrated by modelling, where aspartic acid is presented as red and glycine as blue. b. Inset showing magnification of the amino acid substitution. c. This amino acid change disrupts the native molecular bonds rendering the ensuing mutant unstable.

Fig. 4. a. Substitution of glycine for aspartic acid at position 350 renders the protein thermally unstable as demonstrated across several predictive computational platforms. b. Flexibility analysis using DynaMut suggests p.D350G increases structural mobility.

Fig. 5. a. Immunoblotting of SGPL1 in mutant constructs. Representative Western blot showing lower levels of SGPL1 in p.D350G and other mutant constructs except for p.Y15C, which demonstrated a subtle reduction in protein expression. b. Cortisol output of wild type and SGPL1 KO H295R cell lines after forskolin stimulation. Electrochemiluminescent assay cortisol measurements (normalised to protein content mg/ml) show a robust response in wild type cells when compared to SGPL1-knockout. Markedly less steroid output was obtained from expression of the p.D350G variant when compared to wild type-rescue. Data are presented as the mean ± SD of three repeated measurements (3 independent replicates) (****p<0.0001).

307

308 **Table 1.** The timeline of pertinent clinical features as they occurred.

Age of presentation	Clinical presentation, diagnoses	Biochemistry	Treatment	Radiological findings
9 months	Upper respiratory tract infection, Fever, seizures, hyperpigmentation, ichthyosis Diagnosis – Meningoencephalitis, Primary adrenal insufficiency	WBC: 17.3×10^9/L CRP: 182 mg/L Glucose: 93 mg/dl Na: 136 mmol/L (NR 133-146) K: 4.9 mmol/L (NR 3.5-5.5) BUN: 8 mg/dl (NR 0-23) Creatinine: 0.37 mg/dl (NR 0.6-1.2) ACTH: > 4500 pmol/L (NR 0-103) Cortisol: 0.76 µg/dL (NR 7.2-25) Renin: 54 pg/mL (NR 0.4-33) Aldosterone: 95 pg/mL (NR 70-540) 17 OHP: 0.1 nmol/L (NR <0.1) $DHEASO_4$: <15µg/dL T. Testosterone: < 10 ng/dL Progesterone: <0.1 ng/mL FSH: 4.3 mIU/mL (NR 0-2.4) LH: <0.2 mIU/mL (NR 0-3.8) E2: <5 pg/mL VLCFA levels: Normal	Glucocorticoid and mineralocorticoid replacement, Anti-viral therapy, anti-epileptic therapy	Cranial MRI-Increased bilateral uptake in parieto-occipital leptomeningeal areas
10 years 2 months	Anterior neck swelling		Resection of lesion revealed calcified mass suggestive of thyroglossal cyst	
11 years 5 months	Primary hypothyroidism	TSH: 8.2 mIU/ml (NR 0.6-5.5) Free T4: 10.5 pmol/L (NR 12-24) Thyroid autoantibodies – negative	25 µg/day Na l-thyroxine treatment	Thyroid USS unremarkable
11 years 8 months	Menarche			
13 years				Abnormal pelvic ultrasound scan: Right ovary: one calcification area Left ovary: four calcification areas (maximum calcification area diameter: 7 mm)
16 year 2 months	Routine follow-up	AMH: 4.93ng/ml (NR 0.86-10.45)		Thyroid USS normal.

18

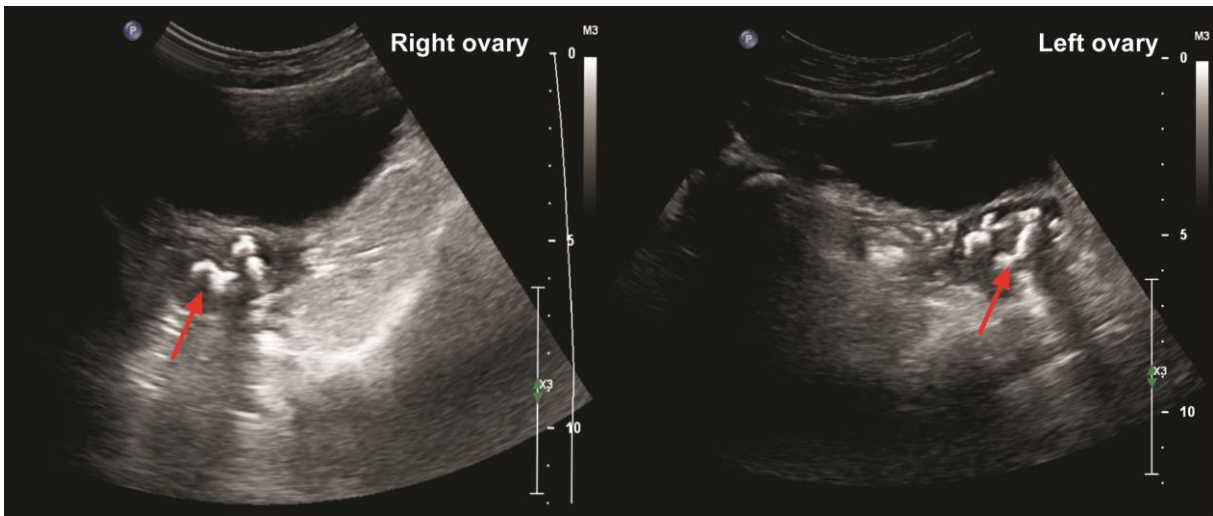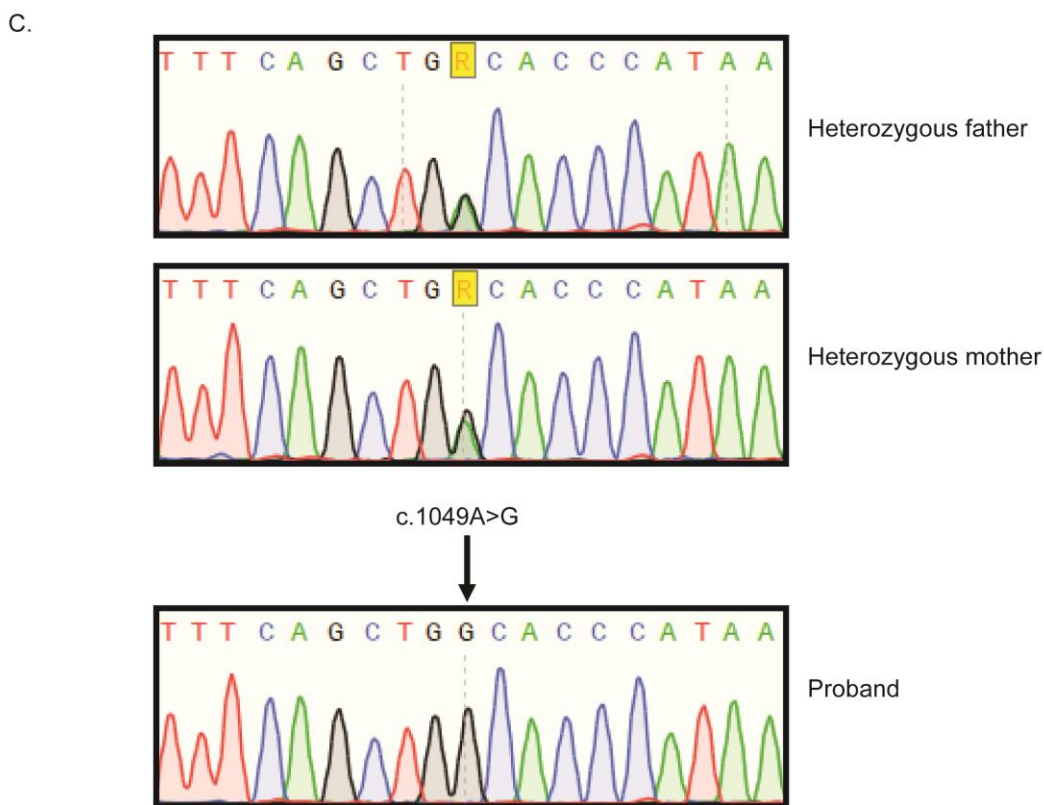|		FSH: 6.04 mIU/ml (NR 1.48-11.7) LH: 23.28 mIU/ml (NR 0.6-21) E2: 112.58 pg/ml (NR 13-71) BUN: 10 mg/dl (NR 0-23) Creatinine: 0.67 mg/dl (NR 0.6-1.2) TSH: 1.848 mIU/ml (NR 0.6-5.5) Triglycerides: 86 mg/dl (NR 35-135)		Ovarian calcifications persist on pelvis USS.

309

310

311   Figure 1
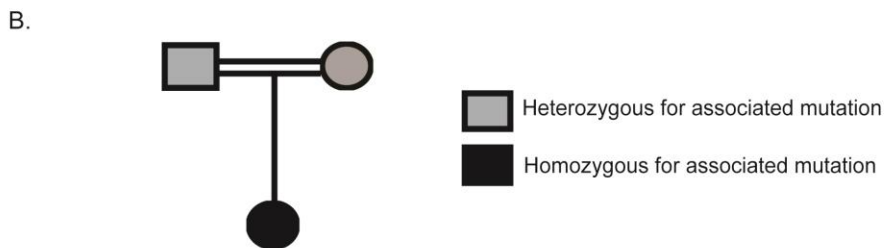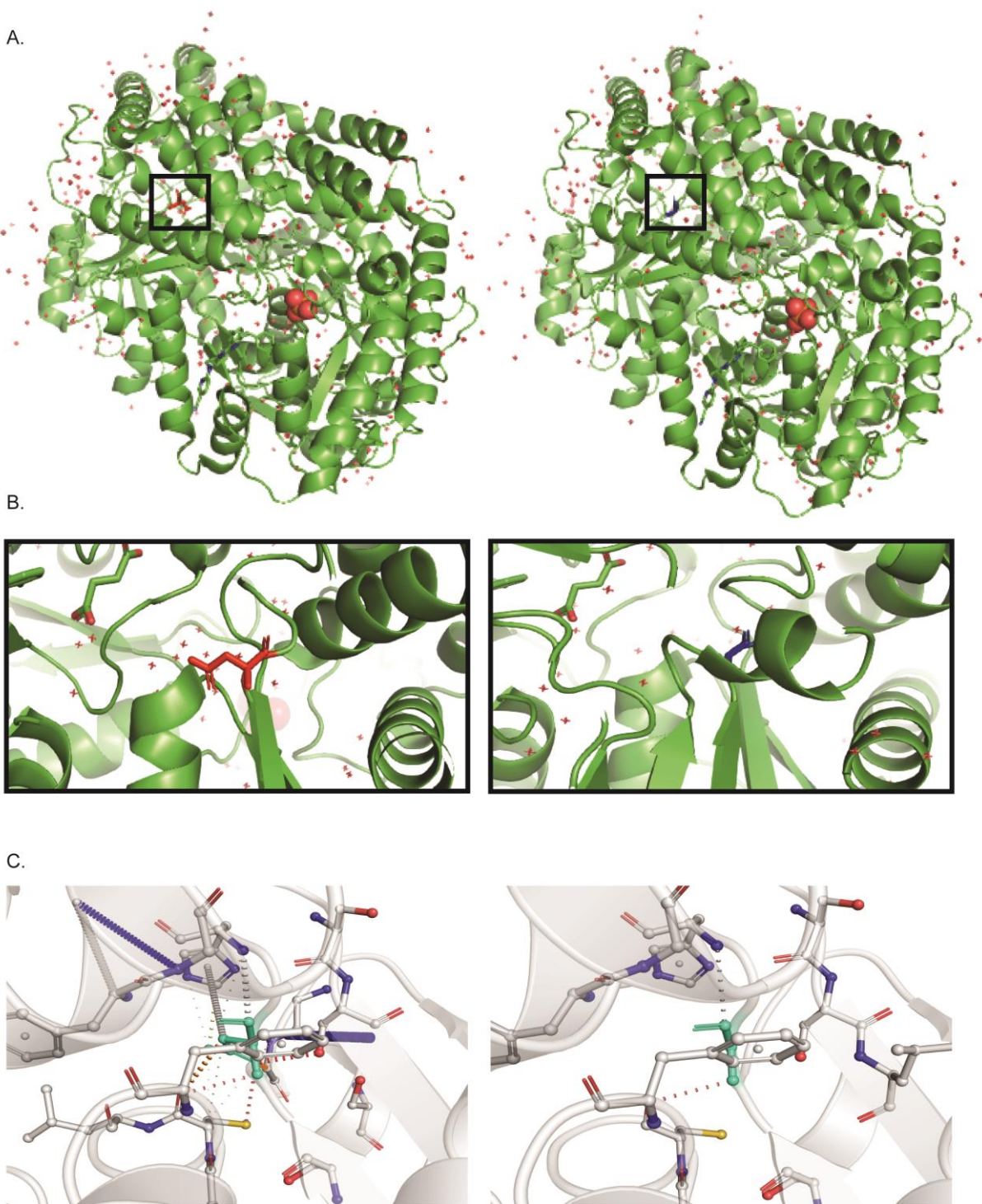

312

313

314

Figure 2

A.

```
O95470 SGPL1_HUMAN   298 VPEVAKLAVKYKIPLHVDACLGGFLIVFMEKAGYPLEHPFDFRVKGVTSISA D THKYGYA 357
Q8R0X7 SGPL1_MOUSE   298 VPEVAKLAVRYKIPLHVDACLGGFLIVFMEKAGYPLEKPFDFRVKGVTSISA D THKYGYA 357
Q8CHN6 SGPL1_RAT     298 IPEVAKLAVKYKIPFHVDACLGGFLIVFMEKAGYPLEKPFDFRVKGVTSISA D THKYGYA 357
A5D788 A5D788_BOVIN  298 IPEVAKLAVKYKIPLHVDACLGGFLIVFMEKAGYPLEQPFDFRVKGVTSISA D THKYGYA 357
E2RME9 E2RME9_CANLF  298 VPEVAKLAVRYKIPLHVDACLGGFLIVFMEKAGYPLEQPFDFRVKGVTSISA D THKYGYA 357
F6XXU8 F6XXU8_HORSE  298 VPEVAKLAVKYKIPLHVDACLGGFLIVFMEKAGYPLEQPFDFRVKGVTSISA D THKYGYA 357
W5P8H8 W5P8H8_SHEEP  298 IPEVAKLAVKYKIPLHVDACLGGFLIVFMEKAGYPLEQPFDFRVKGVTSISA D THKYGYA 357
F1NMD8 F1NMD8_CHICK  279 IEEVAELAVKYKIPFHVDACLGGFLIVFMEKAGFPLKRLFDFRVKGVTSISA D THKYGYA 338
A4QNU7 A4QNU7_DANRE  295 VEEVAKLAVKYNIPFHVDACLGGFLIVFMEKAGFKLA-PFDFRVKGVTSISA D THKYGYA 353
F6RT45 F6RT45_XENTR  246 IEEVAELALKYQLPFHVDACLGGFLIVFMKKAGFPLK-PFDFRVKGVTSISA D THKYGYA 304
                          : ***:**::*::*:***************.***: *  ***********.* *.******
```
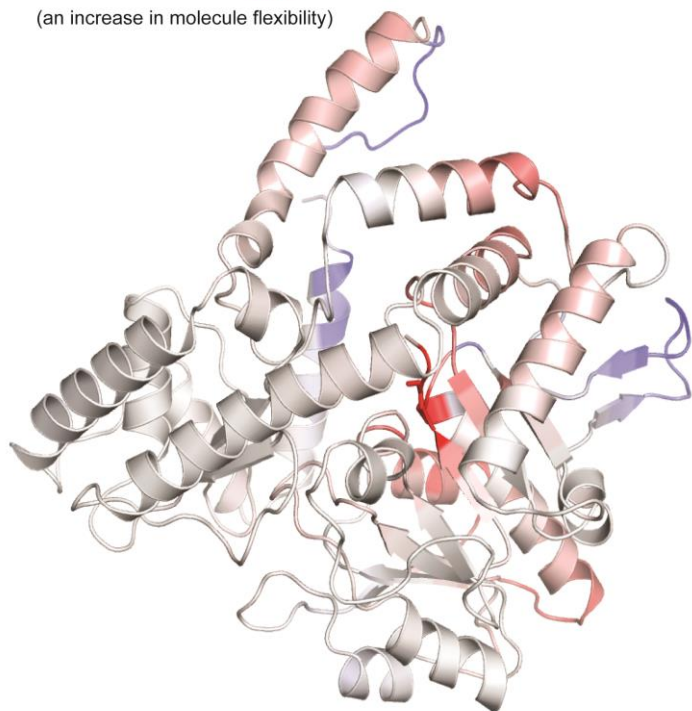
B.

Heterozygous for associated mutation

Homozygous for associated mutation

C.

Heterozygous father

Heterozygous mother

c.1049A>G

Proband

315

316

21

Figure 3

A.

B.

C.

Figure 4

A.

Computational platform	I-Mutant2.0 SEQ	MUpro_SVM	MUpro_NN	iPTREE-STAB	DynaMUT NMA based	SDM
Stability	Decrease	Decrease	Decrease	Decrease	Decrease	Decrease
ΔΔG	-1.16	-1	-0.897	-1.1667	-0.340	-0.83

B.

Δ Vibrational Entropy energy: 0.425 kcal.mol^{-1}.K^{-1}
(an increase in molecule flexibility)

321

322

Figure 5

A.

B.